Thermochimica Acta 519 (2011) 6–11

Contents lists available at ScienceDirect

Thermochimica Acta

journal homepage: www.elsevier.com/locate/tca

Glass-ceramics based on spodumene–enstatite system from natural raw materials

Gamal A. Khater[1], Morsi M. Morsi*

National Research Center, Glass Research Department, Dokki, Cairo, Egypt

ARTICLE INFO

Article history:
Received 22 September 2010
Received in revised form 6 January 2011
Accepted 14 February 2011
Available online 25 February 2011

Keywords:
Glass ceramics
Enstatite
Spodumene
Crystallization
Raw materials

ABSTRACT

Glasses of compositions (wt%) corresponding to 50–90 spodumene and 50–10 enstatite were prepared depending on natural raw materials and Li_2CO_3 as small ingredient. The crystallization behavior was studied using DTA and XRD. The effect of addition of the nucleating agents (LiF) to a selected glass was also examined. Polarizing microscope and dilatometeric techniques were used to study the microstructures and the thermal expansion coefficient, respectively. XRD showed that the crystalline materials are mainly enstatite, clinoenstatite, β-eucryptite ss and β-spodumene ss. The shift of the glass composition to that of enstatite results in increased bulk crystallization. The presence of LiF does not greatly affect the mineral assemblages yet it improves the thermal expansion coefficients (TEC) of the crystalline samples and promotes the initial crystallization. Low and even negative values, ranging from -5.91×10^{-7}/K to 2.48×10^{-7}/K in the temperature range 293–573 K and 300–737 K, respectively, could be obtained, which make such materials applicable for thermally stable articles.

1. Introduction

Extensive investigation has been made on the crystallization of glasses and/or melts based on natural rocks and waste material to obtain new crystalline glass materials (glass-ceramics) from cheap resources. Glass-ceramics are used in a wide range of technical applications, for example, in construction and for domestic purposes, and in the microelectronics industry [1] particularly low expansion glass ceramics which form the most important class of glass ceramics commercially for cook top panels and precision optical applications [2]. Refractory glass-ceramics containing at least 90% by volume enstatite and exhibiting a high modulus of rupture and a use temperature of at least 1200 °C, were developed [3]. Glass-ceramics from local raw materials in the Li_2O–MgO–Al_2O_3–SiO_2 system were prepared and the effects of nucleating agents TiO_2, Cr_2O_3, and P_2O_5 and heat treatment temperature (800 °C, 900 °C, 1000 °C and 1100 °C) on crystallization and morphology were studied [4]. The major phases formed were β-eucryptite and β-spodumene ($LiAlSi_2O_6$), in addition to enstatite and a little anorthite and hematite. Locsei [5] obtained glass-ceramic materials characterized by high wear resistance and chemical durability from glasses based on blast furnace slag, sand and clay with some additions of crystallization catalysts. Khater and Idris [6] studied the crystallization of glasses based on clay, silica sand and some chemical reagents. They obtained crystalline materials composed mainly of spodumene and celsian. Glass-ceramic materials from glasses based on slag, quartz sand, limestone, dolomite, talc, natural raw materials, industrial mining and industrial wastes have also been obtained [7–10]. The nature of the crystalline phases and microstructure of the glass ceramic materials were reported to most important factors affecting the technical properties of the glass-ceramics [11].

Crystal nucleation is a fundamental process of phase formation in glass melts based on molecular level fluctuations under a regime of super saturation. The time and temperature dependent kinetics of crystal nucleation are of crucial importance in determining the glass forming abilities of melts and play an important role in their wide ranging technological applications as glass ceramic materials. Whereas for most devetrifications the composition differ for glass and crystal, a limited number of glass compositions crystallise isochemically, i.e. without changes in composition [12]. Nucleation can occur in such glasses on pre-existing surfaces and in the absence of any initial surface [13]. The nucleation kinetics of the latter process (homogeneous volume nucleation) has been described using the results of the classical nucleation theory [14–17].

Glass ceramics based on the enstatite–spodumene has been chosen for the present study because of, the easy of obtaining their components from natural raw materials that reduce the costs of its preparation. Furthermore, the effect of the nucleating agent LiF has not been studied for such system. The outstanding strength, excellent abrasion, chemical resistance and low thermal

* Corresponding author. Tel.: +20 123733794; fax: +20 23370931.
E-mail address: mmmorsi@yahoo.com (M.M. Morsi).
[1] On leave.

0040-6031/$ – see front matter © 2011 Elsevier B.V. All rights reserved.
doi:10.1016/j.tca.2011.02.021

Table 1
Chemical compositions (wt%) of the raw materials used.

Oxides	Silica sand	Clay	Magnesite
SiO_2	99.50	54.40	3.12
Al_2O_3	0.52	28.20	0.05
Fe_2O_3	0.04	2.33	0.06
TiO_2	–	1.35	0.02
MgO	0.05	0.27	44.60
CaO	0.05	0.26	2.45
Na_2O	0.05	0.58	0.08
K_2O	0.05	0.18	0.02
L.O.I.[a]	–	12.37	49.12

[a] Loss on ignition.

expansion are of the most valuable features of the phases formed in the chosen glasses. Beta-spodumene was considered as a candidate structural material for use in fusion reactor environments, where it has good thermal shock resistance and a very low coefficient of thermal expansion [18]. Beta-spodumene has also exceptional long time dimensional stability at high temperature [19]. Enstatite ceramics are important for its very high melting point, mechanical and electrical properties [20]. The aim of this work is to study the crystallization behavior of some glasses of compositions (wt%) corresponding to 50–90 spodumene and 10–50 enstatite. The effect of the nucleating agent LiF, on the phase assemblages and microstructures and thermal expansion characteristics will also be explored.

2. Experimental procedure

Five glass compositions within the spodumene ($LiAlSi_2O_6$)–enstatite ($MgSiO_3$) system were selected for the present work. These compositions are based on the spodumene composition with successive additions of enstatite up to 50 wt% at 10% intervals of the enstatite component. Natural raw materials (clay, magnesite and silica sand) in addition to some technical chemical reagents such as Li_2CO_3 as a source of Li_2O were used. Table 1 lists the compositions of the used natural raw materials. The details of glass compositions in oxide percentages and percentages of raw materials are given in Table 2. A selected glass (G3) was chosen to add the nucleating agent (LiF). This glass (G3) has an average content of enstatite (30%) in the range of compositions studied (10–50%).

The batches of the compositions under consideration were thoroughly mixed, melted in Pt crucibles in a Globar furnace at temperatures ranging from 1400 to 1450 °C for 2–3 h depending upon the composition. The melts become more viscous for glasses of compositions with high wt% enstatite. The homogeneity of the melts was achieved by swirling the crucible several times at about 20 min intervals. After melting and refining the bubble-free melt was cast onto a steel marver into buttons and rods and transferred to a preheated muffle furnace for stress release.

DTA scans were carried out to determine the crystallization temperatures using a Shimadzu DTG60 microdifferential thermoanalyzer. 40 mg of powdered glass sample, of grain size less than 0.60 mm and larger than 0.2 mm, was used against Al_2O_3 powder as a reference material. A heating rate of 20 °C/min and sensitivity setting of 20 μv/inch were maintained for all the runs.

To induce crystallization using the pre-determined DTA crystallization temperatures, the glass samples were subjected to two different controlled heat treatment processes. The first, was carried out in a muffle furnace from room temperature to the required temperatures (850 or 950 °C) and kept at the intended temperature for 2 h, after which the furnace was switched off and the samples were allowed to cool inside it to room temperature. The second heat treatment processes is a double-stage heat-treatment schedule where glass samples were first soaked at 700 °C for 1 h and then at 950 °C for 2 h.

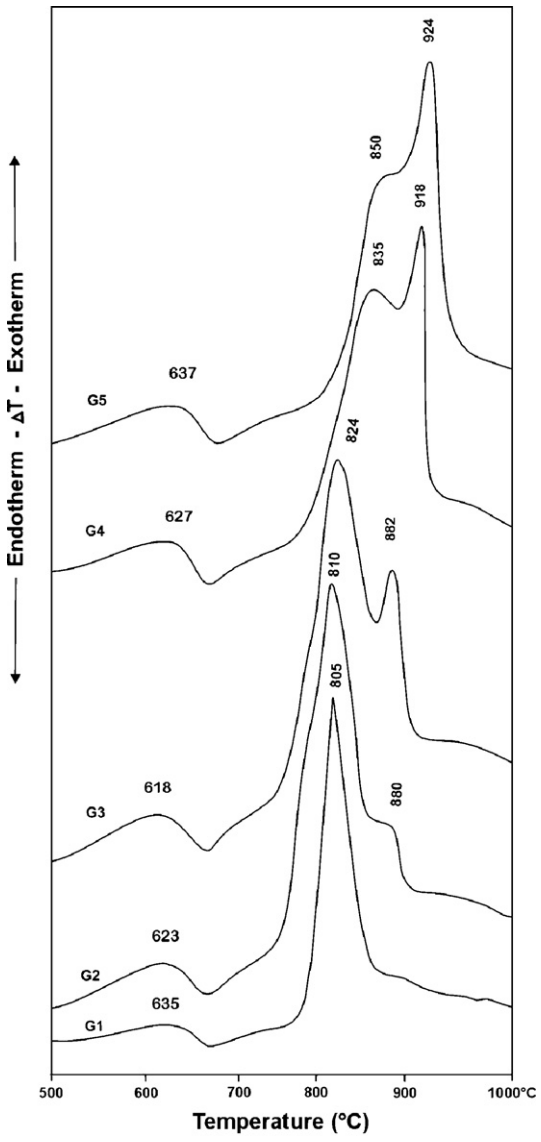

Fig. 1. DTA scans of glasses G1–G5.

The microstructure of almost all the heat treated specimens were examined optically in thin sections using a polarizing Carl Zeiss research microscope.

The crystalline phases precipitated in the course of crystallization was identified by the X-ray diffraction analysis using powdered samples. The X-ray diffraction patterns were obtained using a Bruker D8 Advance, Germany, adopting Ni-filtered CuKα radiation. All the instrument settings were maintained for all the analyses using a Si disk as an external standard.

Measurements of linear thermal expansion coefficients (TEC) of the nucleated glass and corresponding glass-ceramics were carried out using a thermo-dilatometeric analyzer of Netzsch Dil 402 PC, using a fused silica bar as a standard. The thermal expansion of annealed glass rod specimens was measured from room temperature up to temperatures slightly exceeding their dilatometeric softening points. The glass rods were then subjected to thermal treatment and their TEC was measured again from room temperature up to the maximum heat-treatment temperatures. The expansion coefficient (α) was calculated using 5.4×10^{-7} as the correction factor of the quartz tube. The transition temperature (T_g)

Table 2
Compositions and glass transition temperatures of the investigated glasses.

Glass no.	T_g (°C)	Nominal phase* composition (wt%)	Calculated oxide constituents (wt%)				Batch ingredient (wt%)			
			SiO_2	Al_2O_3	Li_2O	MgO	Clay	Silica sand	Li_2CO_3	$MgCO_3$
G1	637	10% Enst. + 90% Spod.	64.10	25.66	7.23	4.02	68.77	10.94	13.49	6.73
G2	627	20% Enst. + 80% Spod.	63.63	21.92	6.42	8.03	58.63	15.83	11.96	13.58
G3	618	30% Enst. + 70% Spod.	63.16	19.18	5.62	12.05	50.57	17.47	10.32	20.09
G4	627	40% Enst. + 60% Spod.	62.68	16.44	4.82	16.06	42.75	14.98	8.37	26.41
G5	632	50% Enst. + 50% Spod.	62.21	13.70	4.01	20.08	35.14	12.49	7.17	32.56
G3L	613	G3 + 1.5% LiF								

* Enst. = enstatite, spod. = spodumene.

and the softening temperature (T_s) of the glass were determined from the expansion curves of the annealed glass.

3. Results and discussion

Differential thermal analysis of the prepared glasses shows (Fig. 1) discontinuities in the baseline of the DTA curves in the range from 618 to 637 °C due to transition temperatures T_g. Exothermic peaks are also recorded in the range from 805 °C to 924 °C indicating crystallization reactions.

According to Fig. 1 T_g decreases, when the content corresponding to enstatite was increased from 10 to 30 wt%, and then increases when the content of enstatite reached 50%. From Table 2 it can be noticed that, SiO_2 is not significantly changes when the content corresponding to enstatite is increased from 10 to 50 wt%. It slightly decreases from 64.10 (glass G1) to 62.21 wt% (glass G5), meanwhile in glasses G1 and G5 the oxides of aluminum and lithium decrease appreciably from 25.66 to 13.70 (wt%) (for Al_2O_3) and from 7.23 to 4.01 (wt%) (for Li_2O). On the contrary, MgO increases drastically from 4.02 to 20.08 wt% in glasses G1 and G5, respectively. It is known that Al^{3+} ion cannot be considered a glass-former by itself, yet it can enter into the structure, in the presence of another ion with a single positive charge to attain electrical balance, to form AlO_4 [21,22]. As a result Al^{3+} in the presence of Li^+ can contribute in the strengthening of the glass structure. On the other hand MgO is reported to contribute to the weakening of silica network and reduce the stability of glass structure [23]. The effect of MgO seems to predominate up to glass G3 as revealed by the shift of T_g towards lower temperature values. It is expected that such behavior will be noticed in glasses G4 and G5, yet the T_g of these glasses showed increased values which may reveal strengthening of the glass structure through the introduction of AlO_4 in the network positions. The increased T_g in such cases is consistent with the visual observation of increasing the viscosity in glasses with composition of high wt% enstatite.

X-ray diffraction (Fig. 2 and Table 3) of glasses treated at 850 °C for 2 h showed that the β-eucryptite ss (ASTM card no. 79-1159), β-spodumene ss (ASTM card no. 13-250), enstatite (ASTM card no. 22-714),and clinoenstatite (ASTM card no. 19-769) are the main crystalline phases developed in these glasses. In sample G1 β-spodumene ss and minor of β-eucryptite ss were formed, and in sample G2 β-eucryptite ss as a major crystalline phase and enstatite were formed. In samples G3–G5 β-eucryptite ss still formed as the major crystalline phase and enstatite is transformed into clinoenstatite. After treatment at higher temperature 950 °C for 2 h, β-eucryptite ss is transformed into β-spodumene ss and enstatite is transformed into clinoenstatite.

Visual examination of glasses G2 and G3 after the double-stage heat treatment showed that crystallization is generally started from the surface of the samples together with the formation of crystalline aggregates in the bulk which are embedded in glassy matrix. Microscopic examination of glasses G2 and G3 after heat treatment shows (Fig. 3) that, the phases crystallized are coarse grained crystals. Fig. 3a shows micrograph of glass G3 (free of catalyst) where relatively non-uniform coarse grained texture of β-spodumene ss and clinoenstatite are developed when it was treated at 700 °C for 1 h and then at 950 °C 2 h (Fig. 3b). Glasses G4 and G5 when heat treated at the same conditions showed by microscopic examination that crystallization proceeded readily throughout the bulk of the sample.

Table 3
X-ray identification of crystalline phases developed in the investigated glasses at selected heat-treatment temperatures.

Glass no.	Heat-treatment parameters (°C, h)	Phases developed[a]
G1	850 °C 2 h	β-Spod. ss + β-euc. ss (minor)
	950 °C 2 h	β-Spod. ss
G2	850 °C 2 h	β-Euc. ss +enst.
	950 °C 2 h	β-Spod. ss +clinoenst.
G3	850 °C 2 h	β-Euc. ss +clinoenst.
	950 °C 2 h	β-Spod. ss + clinoenst.
G4	850 °C 2 h	β-Euc. ss +clinoenst
	950 °C 2 h	β-Spod. ss + clinoenst.
G5	850 °C 2 h	β-Euc. ss + clinoenst.
	950 °C 2 h	β-Spod. ss +clinoenst.
G3L	950 °C 2 h	β-Spod. ss +clinoenst.

[a] β-euc. ss = β-eucryptite solid solution, β-spod. ss = β-spodumene solid solution, enst = enstatite, clinoenst. = clinoenstatite.

The efficiency of the Li_2O on the homogeneous crystallization of the basic oxides in lithium aluminosilicate glasses was attributed to the combination of the high mobility and high field strength of the Li^+ ion [24]. It can be seen from Table 3 that lithium aluminum silicate phases (β-eucryptite ss and/or β-spodumene ss) are the essential crystalline phases that crystallized in all glasses, while enstatite appears in small amounts only at 850 °C and transformed into clinoenstatite at 950 °C. The crystallization in the spodumene rich-glasses (G1–G3) begins at relatively lower temperature with the formation of β-spodumene ss (at 850 °C, e.g. G1). While in case of increased magnesium oxide content (e.g.G2–G5) the β-eucryptite ss was formed at 850 °C and transformed into β-spodumene ss at 950 °C and also enstatite was formed at low temperature at 850 °C and transformed into clinoenstatite at 950 °C. The β-eucryptite ss → β-spodumene ss transformation and enstatite → clinoenstatite transformation needs higher temperature, due to the presence of increasing Mg^{2+} ions in the structure of lithium aluminum silicate phases. These results are in good agreement with those obtained by other authors [25]. McMillan [11] showed that the first detectable crystalline phase was β-eucryptite ss which appeared at about 850 °C, when the temperature was raised above 975 °C the proportion of this phase diminishes fairly rapidly with increasing amounts of β-spodumene ss and appears as the temperature reaches a maximum of 1100 °C. Khater [26] also

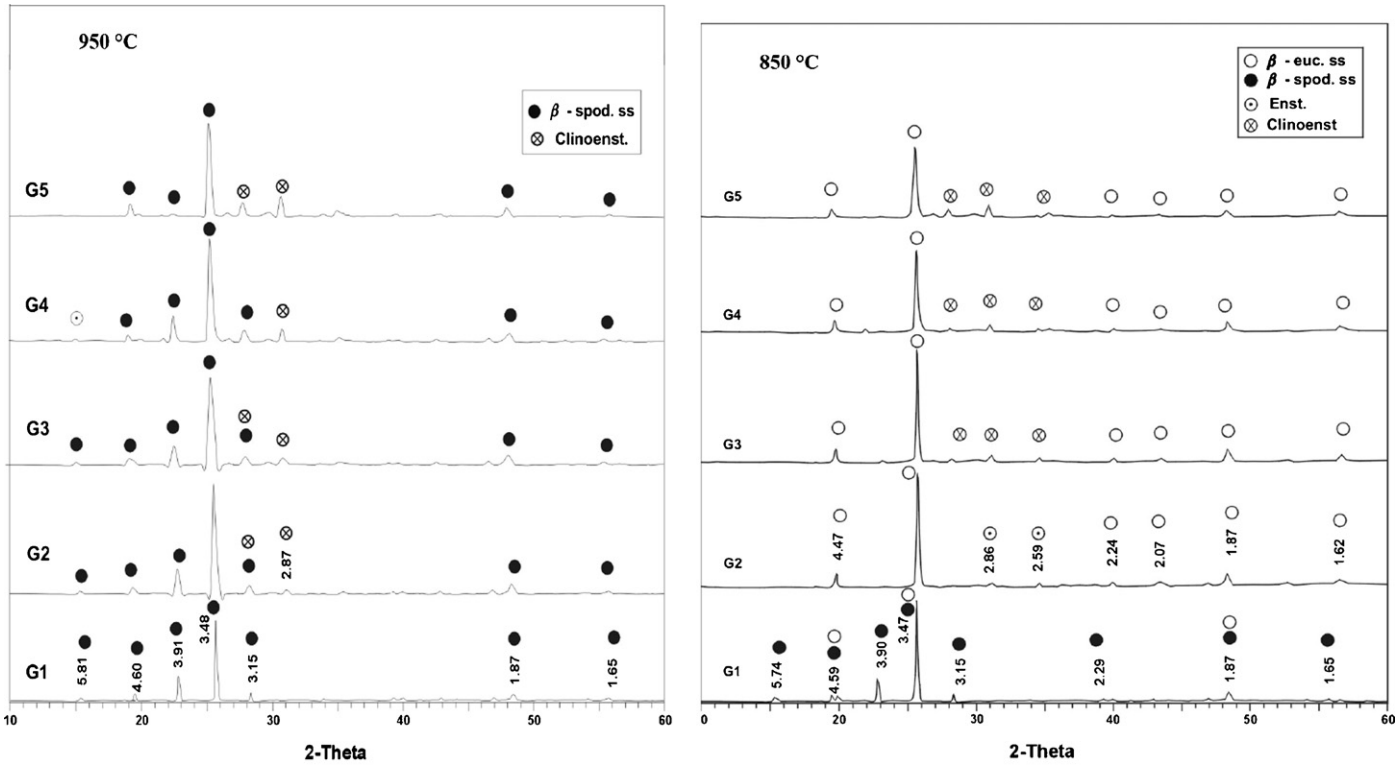

Fig. 2. XRD patterns of samples G1–G5 heat treated at 850 °C and 950 °C for 2 h each.

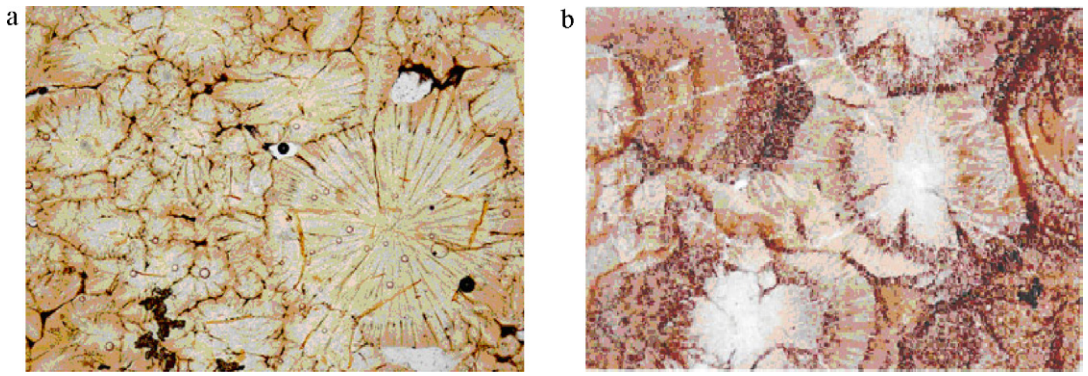

Fig. 3. . Photomicrographs of (a) sample G3 (b) sample G3L heat treated at 700 °C for 1 h followed by 950 °C for 2 h. P.N. 50×.

showed that the crystallization of Li_2O–MgO–Al_2O_3–SiO_2 starts with the formation of β-eucryptite ss which transforms at higher temperature into β-spodumene ss. This transformation temperature depends upon the magnesium content in the glass. In case of high magnesium in the glass, the β-eucryptite ss → β-spodumene ss transformation takes place at high temperatures and long period of times. This is due to the presence of increasing amounts of Mg^{2+} ions in the structure of lithium aluminum silicate phases β-eucryptite ss and/or β-spodumene ss.

Glass G3 was chosen to study the effect of the nucleating agent (LiF) on the mineralogical phases, microstructures formed and thermal expansion coefficient in the resultant crystalline materials. LiF was incorporated in the glass G3 in amount of (1.5 g/100 g glass). The addition of LiF to glass G3L reduced its viscosity as indicated by the reduction of its T_g, compared with that of fluoride-free glass G3, accordingly crystallization is enhanced in G3L. From the DTA (Fig. 4 curve b) the exothermic crystallization peak of glass G3L appeared at lower temperature when compared with that of LiF-free glass G3 (Fig. 4 curve a).

X-ray diffraction analysis (Fig. 5 pattern a and Table 3) showed that the G3 glass (free of catalyst) forms β-spodumene ss and clinoenstatite upon heat treatment at 950 °C for 2 h, also in LiF-containing sample (G3L), β-spodumene ss and clinoenstatite phases are formed when it was treated at the same conditions (Fig. 5 pattern b and Table 3). Although, the phases formed in samples G3 and G3L are of the same kinds, DTA thermograms indicated a difference in the exothermic peak positions for these glass samples (Fig. 4). Exothermic peaks appeared at about 824 °C and 882 °C for glass G3 and at about 770 °C for glass G3L. This difference confirms the enhancement effect of LiF on the crystallization of β-spodumene ss and clinoenstatite phases. Microscopic examination of the heat-treated nucleated glass shows that the LiF additions has little effect on the nucleation process and develops coarse-grained textures when it was treated at 700 °C for 1 h and then at 950 °C for

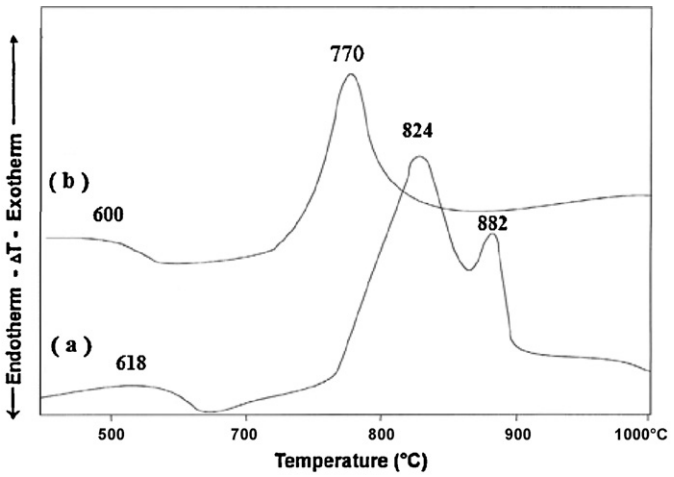

Fig. 4. DTA curves of (a) G3 glasses without additives and (b) glass G3L with 1.5 g LiF/100 g glass.

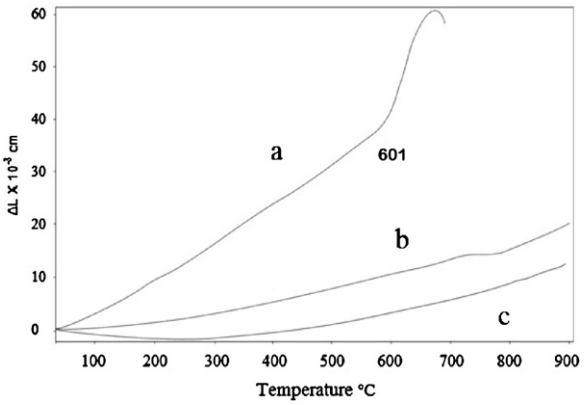

Fig. 6. Thermal expansion coefficient of (a) glass G3L, (b) glass G3L heat treated at 850 °C for 2 h and (c) glass G3L heat treated at 950 °C for 2 h.

Table 4
Heat treatment conditions and mean thermal expansion coefficient of glass G3L containing 1.5 g LiF/100 g glass.

Temperature (°C, h)	Mean TEC (10^{-7}/K)		Phases developed
	20–300 °C	300–500 °C	
As prepared[a]	58.90	67.12	Amorphous
850 °C, 2 h	10.83	16.36	β-Euc. ss + enst.
950 °C, 2 h	−5.91	2.48	β-Spod. ss +clinoenst.

[a] The glass has T_g = 601 °C, and T_s = 682 °C as estimated from TEC.

2 h (Fig. 3b). Similar results were recorded [27] where fluorine was found to promote the crystallization of β-spodumene and increases the crystal size in Li_2O–Al_2O_3–SiO_2 glass ceramic.

The dilatometric curves of G3L glass and its corresponding glass-ceramics are shown in Fig. 6. Table 4 lists the thermal expansion coefficients (TEC) over different ranges, the heat treatment parameters and the developed crystalline phases. From Fig. 6 it can be noticed that G3L has linear expansion coefficient (58.9×10^{-7}/K) higher than that of sample containing LiF (G3L) heat treated at 850 °C for 2 h (10.83×10^{-7}/K) or that of G3L heat treated at 950 °C for 2 h (-5.91×10^{-7}/K). Fig. 6 also shows that, T_g for glass G3 is about 601 °C which is very close to that (600 °C) estimated from DTA (Fig. 4).

The effect of addition of lithium fluoride to glass G3 on the crystallization behavior can be outlined as follows: It is reported that fluorine promotes nucleation and crystallization and decreases the melting temperature of silicate glasses [28,29] through the decrease of crosslinking in the glass network [30]. These findings are consistent with the observed shift of the transition temperature T_g (618 °C) of glass G3 towards lower T_g temperature (600 °C) for glass G3L, and the shift of the crystallization temperatures from 824 °C and 882 °C to 770 °C upon the addition of LiF (Fig. 4).

Thermal expansion coefficient is a function of the thermal expansion coefficients and elastic properties of all formed phases, including residual glass. The mean thermal expansion coefficients of glass-ceramics particularly influenced by the nature and concentration of the crystalline phases formed. Fig. 6 shows that the mean expansion coefficient of the LiF-containing glass-ceramics treated at 850 °C for 2 h (Fig. 6 curve b) have higher value than that treated at 950 °C for 2 h Fig. 6 (curve c). The difference in linear expansion coefficient of both heat treated glass samples may be attributed to different amounts of the crystallized phases. However, the low and even a negative CTE of glass-ceramic materials of this system can suggest their application in stove, cookware, and some precision thermally stable parts [31,32].

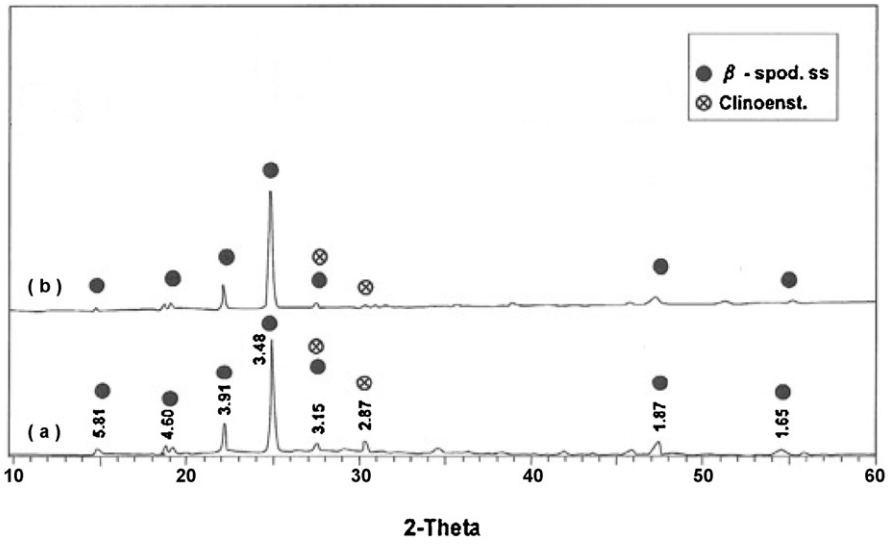

Fig. 5. XRD patterns of (a) glass G3 without additives and (b) G3L with LiF.

4. Conclusions

The crystallization sequence in glasses of compositions corresponding to (wt%) 50–90 spodumene and 10–50 enstatite begins with the formation of metastable β-eucryptite ss followed by, or concurrent with the crystallization of enstatite. By the increase of the temperature a rapid transformation of β-eucryptite ss → β-spodumene ss and enstatite → clinoenstatite. Low mean values of TEC could be obtained for glass ceramics with 30% enstatite and 70% spodumene and containing 1.5 g LiF/100 g glass. The TEC are ranging from -5.91×10^{-7}/K to 2.48×10^{-7}/K in the temperature range 293–573 K and 300–737 K, respectively. The present glass ceramics are promising materials to be used in industry for domestic purposes.

References

[1] G. Partridge, Glass Technol. 35 (1994) 171–182.
[2] P. Wolfgang, Glastech. Ber, Glass Sci. Technol. 73 (C1) (2000) 21–27.
[3] G.H. Beall, US Patent 4687749, Publication date: 08/18/1987 (1987).
[4] O.A. Al-Harbi, M.M. Khan, Emirates, J. Eng. Res. 13 (2008) 53–59.
[5] B. Locsei, Symposium on Nucleation and Crystallization in Glasses and Melts, American Ceramic Society, Ohio, 1962, pp. 71–74.
[6] G.A. Khater, M.H. Idris, Ind. Ceram. 24 (2004) 43.
[7] G.A. Khater, Glass Technol.: Eur. J. Glass Sci. Technol. A 51 (2010) 6.
[8] G.A. Khater, J. Non-Cryst. Solids 356 (2010) 3066.
[9] A. El-Maghraby, M.A. Abou-Elmaaty, G.A. Khater, N.Y. Mostafa, J. Am. Sci 6 (2010) 691.
[10] G.A. Khater, E.M.A. Hamzawy, Ceram. Trad. 1 (2010) 15.
[11] P.W. McMillan, Glass-Ceramic, 2nd edition, Academic Press, London, 1979.
[12] P.F. James, Ceram. Transact. 30 (1993) 3.
[13] R. Müller, E.D. Zanotto, V.M. Fokin, J. Non-Cryst. Solids 274 (2000) 208.
[14] P.G. Debenedetti, Metastable Liquids: Concepts and Principles, Princeton University Press, Princeton, 1996.
[15] J. Frenkel, Kinetic Theory of Liquids, Oxford University Press, Oxford, 1946.
[16] A. Laaksonen, V. Talenquer, D.W. Oxtoby, Ann. Rev. Phys. Chem. 46 (1995) 489–524.
[17] P.M. Chaikin, T.C. Lubensky, Principles of Condensed Matter Physics, Cambridge University Press, Cambridge, UK, 1995, pp. 479–491.
[18] P.V. Kelsey Jr., R.E. Schmunk, S.P. Henslee, Conference: Fusion Reactor Materials Meeting, Seattle, WA, USA, August 9, 1981.
[19] R.F. Reade, US Patent 4126477, Publication date: 21/11/1978 (1978).
[20] W.E. Lee, A.H. Heuer, J. Am. Ceram. Soc. 70 (1987) 349–360.
[21] W.A. Weyl, Colored Glass, Society of Glass Technology, 1965, pp. 36–37.
[22] M.C. Wang, C.W. Cheng, P. Yu Shih, C.S. His, J. Non-Cryst. Solids 353 (2007) 2295–2300.
[23] L. Yu, H. Xiao, Y. Cheng, Ceram. Int. 34 (2008) 63–68.
[24] S. Urens, Proceedings of the Sixth Conference on the Silicate Industry, Budapest, October, 1961, pp. 437–443.
[25] H. An-Min, L. Kai-Ming, P. Fei, W. Guo-Liang, S. Hua, Thermochim. Acta 413 (2004) 53–55.
[26] G.A. Khater, MSc thesis, Ain Shams University, Cairo, Egypt, 1987.
[27] X. Guo, H. Yang, C. Han, F. Song, Thermochim. Acta 444 (2006) 201–205.
[28] X. Guo, H. Yang, Mater. Res. Bull. 41 (2006) 396–405.
[29] S.N. Salama, S.M. Salman, H. Darwish, Ceramics-Silikáty 46 (2002) 5–23.
[30] G.S. Painter, P.F. Becher, H.J. Kleebe, G. Pezzotti, Phys. Rev. 65 (2002) 1–11.
[31] H. Scheidler, E. Rodek, Am. Ceram. Soc. Bull. 68 (1989) 1926.
[32] Z. Strnad, Glass-ceramic Materials, Elsevier, Amsterdam, The Netherlands, 1986, p. 182.